

# Geochemical processes in the formation of ‘forest rings’: examples of reduced chimney formation in the absence of mineral deposits

Kerstin Brauner<sup>1\*</sup>, Stewart M. Hamilton<sup>2</sup> & Keiko Hattori<sup>1</sup>

<sup>1</sup> University of Ottawa, Department of Earth Sciences, Ottawa, ON, K1N 6N5, Canada

<sup>2</sup> Ontario Geological Survey, 933 Ramsey Lake Road, Sudbury, ON, P3E 2G9, Canada

\* Correspondence: kbrauner@gmail.com

**Abstract:** Forest rings are large circular features common in boreal forests in Ontario, Canada, characterized by ring-shaped topographic depressions in carbonate-rich soil. This paper documents the compositional variation of soil and of the peat that commonly fills the depression, along transects across two representative rings: one centred on an accumulation of CH<sub>4</sub> in glacial sediments and the other on H<sub>2</sub>S in both glacial sediments and bedrock. Clayey mineral soil at the ring edge (annulus) shows low pH, oxidation-reduction potential (ORP), Ca and carbonate, and high Al, Fe and Mn by both *aqua regia* digestion and a 0.25M hydroxylamine hydrochloride leach (0.25M NH<sub>2</sub>OH.HCl at 60°C). Antithetic responses occur in the overlying peat, including elevated carbonate and pH over the areas with low pH, ORP and carbonate in the mineral soil. The observed relationships suggest vertical migration of carbonate species from mineral soil into peat at the annulus, and lateral migration from the annulus to adjacent areas in the mineral soil. The geochemical data support the hypothesis that forest rings are the surface expression of reduced chimneys, similar to those observed over metallic mineral deposits, despite both these sites being known to be barren. Strongly negative ORP values in shallow soils in the annulus suggest autotrophic microbiological activity contributes to the sharp change in redox conditions at the ring boundaries. The similar geochemical responses at forest rings and soils over mineral deposits show that these features can be used to understand the variation in redox, pH, metals and soil hydrocarbons over mineral deposits and to help differentiate ore-related from secondary geochemical features due to the presence of a reduced chimney.

**Keywords:** reduced chimney; metal transport; H<sub>2</sub>S; CH<sub>4</sub>; redox; autotroph; soil hydrocarbon; false anomaly; geochemical exploration; forest ring

**Received** 26 March 2015; **revised** 29 September 2015; **accepted** 26 October 2015

Forest rings are light-coloured circular imprints in the boreal forest common to northern Canada, ranging in diameter from 50 to 1.6 km. They are visible from aircraft, and on air photos (Fig. 1) and satellite images, because of circular zones of sparse tree density (Fig. 1). The ring edge (annulus, 10–20 m in width) is commonly a poorly-vegetated bog with a slight topographic depression. Over 2000 forest rings have been identified in northern Ontario and Québec since 1999. Previous work on forest rings in Canada established that: (1) they are abundant above glacio-marine and marine sediments and commonly occur over Phanerozoic limestone terrain (Veillette & Giroux 1999; Hamilton *et al.* 2004a), (2) they are visible because of poor tree growth or high tree mortality, spatially coinciding with a depression filled with peat in carbonate-rich soils (Giroux *et al.* 2001), and (3) reduced gases, such as H<sub>2</sub>S (Hamilton & Hattori 2008) and CH<sub>4</sub> (Hamilton *et al.* 2004a) occur in the centre of 11 surveyed forest rings. No detailed studies have documented soil geochemical conditions in the shallow sub-surface of a forest ring.

This paper reports soil geochemical data (pH, redox, carbonate content and metal abundance) from two forest rings with emphasis on the changes at ring edges and discusses the processes forming forest rings partly using principal component analysis (PCA). The two rings selected for this study are the ‘Bean’ ring, centred on an accumulation of CH<sub>4</sub> in overburden (Hamilton *et al.* 2004a) and the ‘Thorn North’ ring, which has elevated H<sub>2</sub>S<sub>(aq)</sub> in groundwater inside the ring (Hamilton & Hattori 2008). Both sites exhibit reducing conditions in groundwater inside the ring, relative to background areas, with Eh

rising sharply at the ring edges. They also display similar soil geochemical patterns to some observed over mineral deposits. These two factors led Hamilton & Cranston (2000) to propose the rings were ‘reduced chimneys’, analogous to those that occur over some mineral deposits. However, they are known from drilling to not be underlain by any buried mineral deposit and the observed geochemical patterns in soils may merely be due to the starkly different Eh (and pH) conditions inside the ring. The primary substances known to be oxidizing at these two sites (H<sub>2</sub>S and CH<sub>4</sub>) would not leave direct chemical products in soils but the processes related to their oxidative change would leave various signals such as acidification, carbonate dissolution-precipitation, and metals deposition.

Therefore one of the objectives of this study is to identify soil geochemical variations related strictly to the presence of reduced chimneys. This information will help differentiate ‘secondary’ geochemical responses over mineral deposits (Hamilton 2000) from primary ore-related responses, which is currently a major challenge in exploration geochemistry.

## Background

Forest rings have been known anecdotally in Ontario since aerial photography became available in the 1950s. The term *forest ring* was applied by the Ontario Geological Survey (Hamilton *et al.* 1999; Hamilton & Cranston 2000), in order to differentiate them from ‘fairy rings’, which are metres-scale rings caused by fungal growth (Gregory 1982) that occur in grasslands, forests and

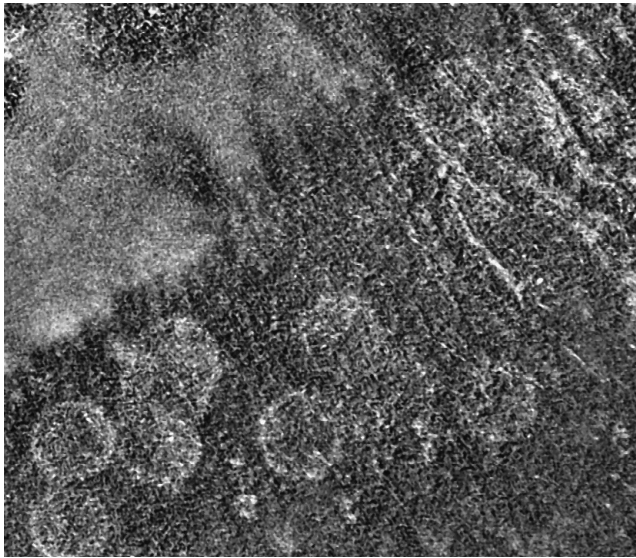


**Fig. 1.** Aerial photograph of forest rings with diameters of approximately 150 m in northern Ontario. The annulus is visible due to stunted tree growth, and preferential growth of moisture-tolerant tree species, such as tamarack. The photograph is located near Latitude 49.49°; Longitude -80.09° and these rings are visible also on satellite images, including those of Google Earth®.

suburban lawns. Previous designations included 'circular ring features' (Pinson 1979), 'giant circular patterns' and 'whitish rings' (Giroux *et al.* 2001). In addition to northern Ontario, 200 rings have been identified over limestone on Anticosti Island in the St Lawrence River (Dubois 1994). Their abundance in northern Ontario is unmatched with over 2000 forest rings identified within a study area of 150 000 km<sup>2</sup>, in the central part of northeastern Ontario (Hamilton *et al.* 2004a).

Early studies proposed a biological origin based on morphology (e.g. Mollard 1980), where forest rings form by radial growth of fungi within the Black Spruce root system. Usik (1966) first suggested forest rings as the surface expression of element dispersion above mineralization. Prospectors have often believed them to be the surface expression of buried kimberlites or other circular features of economic interest (e.g. Millar 1973; Reed 1980; Adams 1998; Diatreme Explorations 1999), but drilling in several forest rings, including the two described in this paper, failed to intersect mineral deposits. Other suggested origins of forest rings are related to relic permafrost features, thermokarst and periglacial features (Mollard 1980).

Studies by Veillette & Giroux (1999) and Giroux *et al.* (2001) used dendrochronology to disprove the biological origin of forest rings. They demonstrated that the trees are the same age on both sides of the ring annulus and therefore the key requirement for radial growth, which is younger trees inside the ring, is not supported. Giroux *et al.* (2001) noted a decrease in elevation of the mineral substrate at the ring edge by up to 3 m, coinciding with changes in forest productivity and concluded that these are geological features, regardless of their underlying cause. Based on the spatial correlation between rings and calcareous substrate, Veillette & Giroux (1999) hypothesized the ring edge depression to be caused by geologic processes at depth related to carbonate. The size of the depression and the thick infill of peat suggest their existence for a long time (Hamilton *et al.* 2004a).

Hamilton & Hattori (2008) presented evidence that forest rings are the surface expression of reduced chimneys, similar to those over concealed mineral deposits (Hamilton *et al.* 2004b, c). Reduced chimneys, or 'columns', (Hamilton 1998; Klusman 2009) are postulated to form over buried sources of negative charge, which maintain overlying sediments and groundwater in a reduced state. Groundwater in glacial sediments at both rings discussed in detail here has been previously shown (Hamilton & Cranston 2000; Hamilton & Hattori 2008) to be chemically reducing (Fig. 2). Groundwater in overburden and bedrock inside the ring at Thorn North is characterized by elevated H<sub>2</sub>S and low oxidation-reduction potential (ORP) that rises sharply at the ring edge. Similarly reducing conditions exist in groundwater at the Bean ring, although it is characterized at a lower sample density (Fig. 2). Hamilton *et al.* (2004a) found elevated methane (CH<sub>4</sub>) in groundwater, fine-grained glacial tills, and glaciolacustrine and glaciomarine clays inside 11 forest rings, relative to outside. One of these was the Bean ring, where they determined isotopically that the methane in overburden is biogenic in origin. These findings and the sharp changes in redox conditions prompted us to examine the geochemical processes at the ring edge.

### Study area

Two forest rings in northeastern Ontario were selected for detailed investigation: the Bean and Thorn North rings (Fig. 3). They were selected from 14 forest rings previously investigated by the Ontario Geological Survey (OGS; Hamilton *et al.* 2004a), because they represent two different types of forest rings: those centred on CH<sub>4</sub> and H<sub>2</sub>S. Furthermore, the two can be easily accessed and have previously installed infrastructure, including monitoring wells. Sampling was carried out in 1999 and 2000.

Previous studies (Hamilton & Cranston 2000; Hamilton *et al.* 2004a; Hamilton & Hattori 2008) using groundwater geochemical

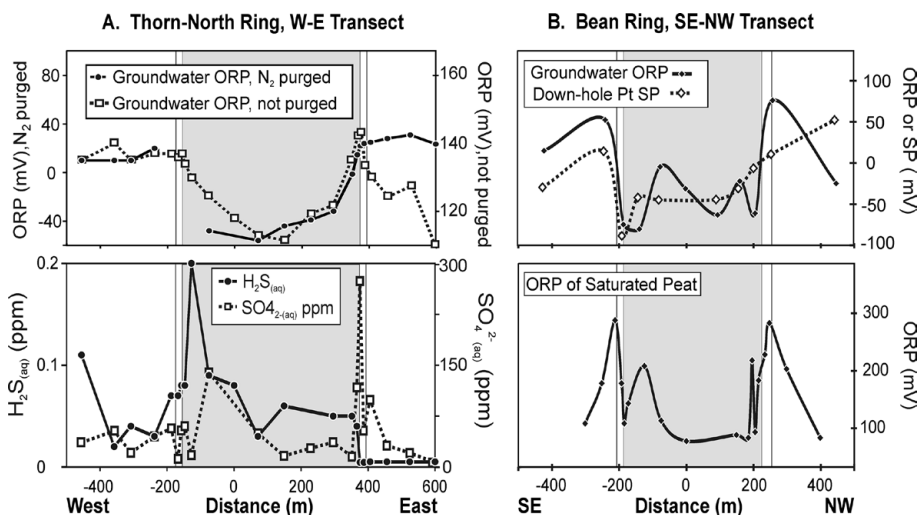


**Fig. 2.** Redox-sensitive parameters in soils and groundwater indicating reduced chimney conditions in glacial overburden at two Forest Rings. (A). Thorn North: groundwater ORP at 8 m depth by two methods (top) and H<sub>2</sub>S<sub>(aq)</sub> and SO<sub>4</sub><sup>2-</sup><sub>(aq)</sub> in groundwater (bottom) (modified after Hamilton & Hattori 2008), (B) Bean: groundwater ORP and down-hole platinum SP (top) referenced against a central Cu-CuSO<sub>4</sub> electrode and ORP of saturated peat collected at 40 cm depth (bottom) (modified after Hamilton & Cranston 2000).

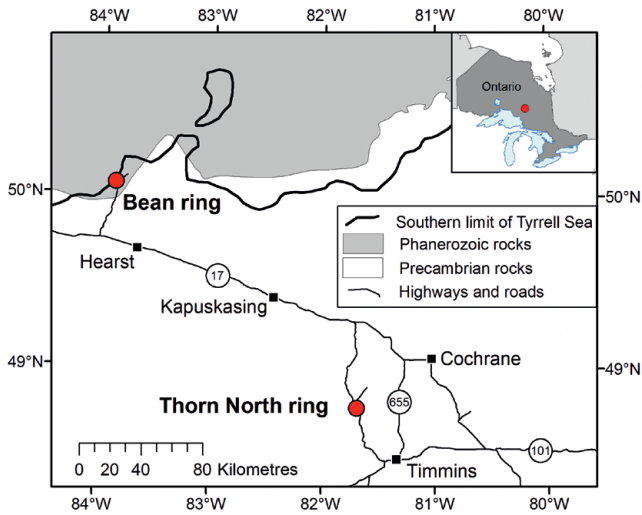


**Fig. 3.** Location of the Bean and Thorn North forest rings (large circles) in northeastern Ontario. Major towns are shown as solid squares. The southern limit of Tyrrell Sea marine incursion is shown as a thick black line.

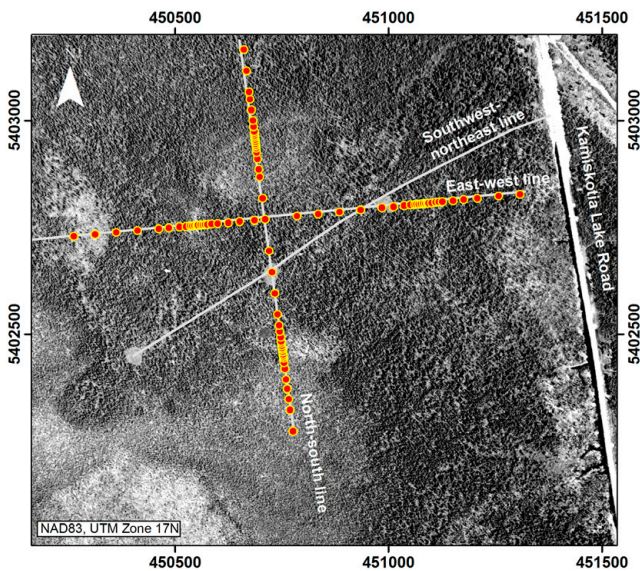


**Fig. 4.** Site map showing the north-south (TN-NS) and west-east (TN-WE) transects of the Thorn North ring, 21 km north of Kamiskotia Lake, NW of Timmins, Ontario. Geo-positioning of the air photo is estimated to be accurate to  $\pm 5$  m. Geo-positioning of the sample points is  $\pm 1$  m, although their accuracy relative to one another is  $\pm$  several centimetres.

and other techniques, identified both these rings as the visual expression of circular 'reduced chimneys' (Fig. 2). Redox conditions in groundwater and soils are distinctly reduced inside relative to outside the rings, and rise sharply at the ring edges.

The area is part of the Abitibi plains eco-region, the boreal-shield climate zone and the boreal forest biome. The vegetation cover is dominated by black spruce, balsam fir and tamarack (a Larch) growing on a thick horizon of well decomposed organic matter (peat). The region has a continental climate, characterized by long cold winters and short warm summers. Timmins, a nearby city, has average temperatures that range from  $-17.2^{\circ}\text{C}$  in January to  $+17.3^{\circ}\text{C}$  in July and total annual precipitation of 831.3 mm ([http://www.climate.weatheroffice.ec.gc.ca/climate\\_normals/index\\_e.html](http://www.climate.weatheroffice.ec.gc.ca/climate_normals/index_e.html)). The Bean ring is located approximately 100 km south, and the Thorn North ring approximately 250 km south, of the boundary of discontinuous permafrost (Smith & Burgess

2002). However, during August sampling, ice was noted in peat on two sites at the centre of the Bean ring. Ice was also encountered at the edge of the Thorn North ring in August (Brauner *et al.* 2008).

Soil development is poor on both sites. Instead of a full B-horizon, parent material (mostly clay) is either unoxidized or shows mild orange or mottled orange/grey texture, which is a common occurrence in intermittently water-logged soils.

### The Thorn North ring

The Thorn North ring (Fig. 4) is located 40 km NW of the city of Timmins (Fig. 3) and has a diameter of 560 m. It is one of the best studied rings due to its road-accessibility. Bedrock consists of Archean igneous rocks of the Superior Province. Drilling encountered quartz-feldspar porphyry with minor (*c.* 1 vol. %) pyrite and chalcopyrite near the centre of the ring, and an intensely sheared rock of the same lithology in a second hole 50 m away (Hamilton & Hattori 2008).

Quaternary sediments were deposited during a period of glacial retreat beginning about 9.4 kA (Dyke 2004). The most widespread deposits consist of an up to 30 m thick varve clay unit that was deposited during the development of proglacial lakes Barlow and Ojibway. Lake Ojibway is the northward succession of Lake Barlow and started forming at 9 kA. A brief 450 year-long re-advance of glaciers began around 8.4 kA (Dyke 2004) during a cold period known globally as the '8.2 K Event'. The Cochrane till was formed as part of this event by glacial over-riding of the glaciolacustrine deposits. Esker deposits are also likely relicts from this glacial re-advance. Near-shore sands on the Thorn North site (Fig. 5) formed in a brief period when lake Barlow-Ojibway prograded northward as the ice started receding again. The lake began draining at 7.6 kA following the opening of an outlet northward into the Tyrrell Sea. Peat has been forming in the area since that time.

The glacial stratigraphy of the Thorn North ring (Fig. 5) was previously described by Hamilton & Hattori (2008) based on 54 8-m deep hollow-stem auger holes. Three additional holes were drilled to bedrock; one outside and two inside of the ring. Glacial drift thickness is approximately 30 m. The Thorn North ring is located on the western margin of a south-SE-trending esker (Paulen & McClenaghan 1998). The eastern 40% of the ring is underlain by fine to medium sand and the western 60% by glaciolacustrine clay and clayey till. Three sampling transects were named after the abbreviated ring name (TN) and their orientation: TN-NS (north-south transect), TN-WE (west-east transect) and TN-SWNE (SW-NE transect; Fig. 4), although the latter was not sampled in its entirety and is not discussed in detail here.

The top organic horizon is composed of peat in most areas and humus in the westernmost 5 sites and easternmost 3 sites on TN-WE (Fig. 5). Organic samples were classified based on visual examination and range from poorly to well humified. Poorly humified samples are partially decomposed, fibrous light to medium brown with well discernible stems and roots ( $O_f$  horizon). Well humified samples are extensively decomposed, soft, and homogeneous dark-brown in colour ( $O_h$  horizon). The uppermost clay is unoxidized on the central part of TN-WE (Fig. 5) and on the entirety of TN-NS. Where oxidation occurs on TN-WE it is marked by an orange/reddish mottling. This unit was referred to as the 'interface unit' at Thorn North on Figure 5 and was distinguished from the deeper uniform-grey clay unit and sampled as a different horizon. Only the deeper data, usually representing uniform-grey unoxidized clay, are discussed, along with the peat data. Field data for the collected peat and soil samples at Thorn North (and Bean) are reported in Brauner (2012). These include sam-

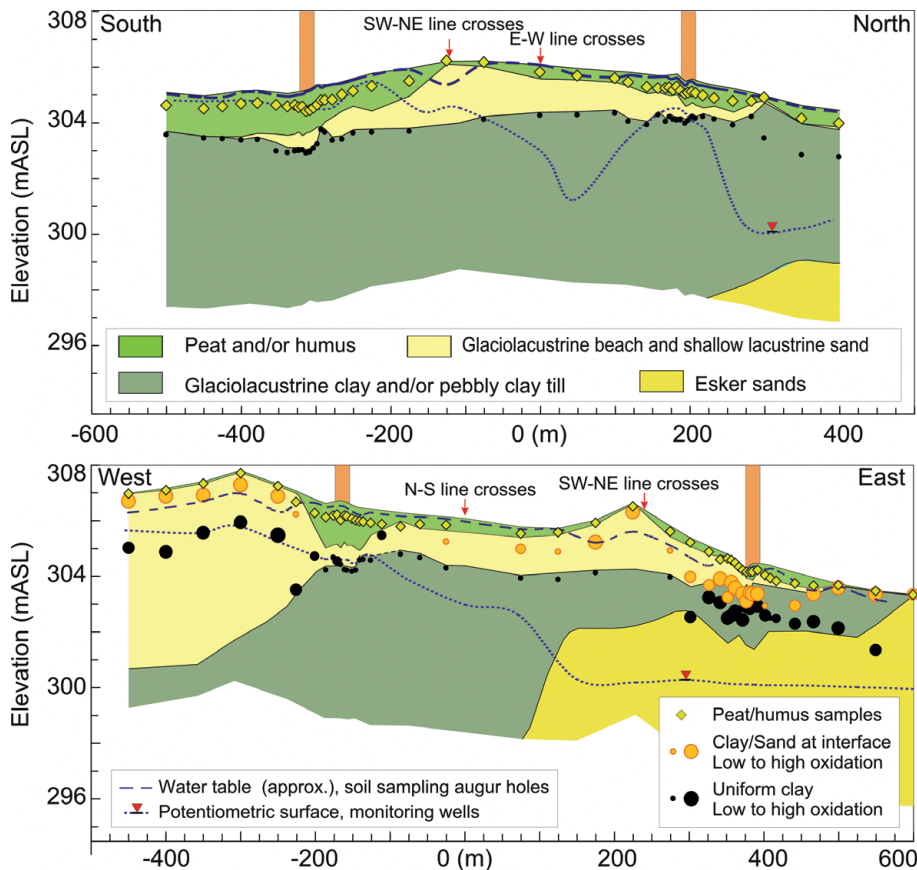


**Fig. 5.** Shallow stratigraphic section and soil sample locations at the Thorn North forest ring for the TN–SN and TN–WE sampling transects. The stratigraphy and potentiometric surface were determined from 54 monitoring wells with well screens at 8–9 m depth. The water table was determined based on the position of standing water in the auger-holes. Different sample media and their variable state of oxidation made the TN–WE transect less useful in this study. Thick vertical bars indicate the position of ring edges. Note the large vertical exaggeration (modified after Hamilton & Hattori 2008).

pling depth, transect location, water depth at the sampling site, the surveyed topography and a short sample description.

Hamilton & Hattori (2008) measured  $H_2S$  in groundwater at most of the shallow wells at Thorn North (Fig. 2). Far higher concentrations of  $H_2S$  occur in water inside than outside of the ring and the change is sharp at the ring edges. Water from two wells that penetrate the sheared quartz-feldspar porphyry, had concentrations of  $H_2S$  up to 2.25 and 11.0 mg/L, which are higher than the 0.35 mg/L measured in groundwater in overburden just above gabbroic rocks in a borehole outside of the ring (Hamilton & Hattori 2008) and therefore the source of  $H_2S$  is likely in bedrock.

The TN–SN transect is wet (Fig. 5) with a shallow water table lying between surface and 0.2 m beneath the surface except in a small, unsampled part near the centre of the transect. Moisture conditions along the TN–WE transect are variable, with the depth of the water table ranging between surface and 1 m. The water table is deepest, ranging between 0.5–1 m, at the centre and the western end of the transect. At these locations the uppermost layer of peat and lacustrine sand are unsaturated and oxidized (Fig. 5).

### The Bean ring

The Bean ring is located within the James Bay Lowlands in Phanerozoic limestone terrain, close to the boundary with Archean rocks (Fig. 3). Drilling in 1999 confirmed the presence of thickly bedded non-fossiliferous micritic limestone as bedrock and showed that the Quaternary sediments (<30 m in thickness) consist largely of stony clay, carbonate-rich (*c.* 35 wt%) till of the Cochrane Formation till, with numerous sand lenses. This till originated as glacially-overridden glaciolacustrine clays. The Bean ring is located outside and within several kilometres of the southern limit of the Tyrell Sea incursion (Fig. 3). Glacial sediments in this part of the James Bay lowlands are thought to be 8.5 ka in age (Dyke 2004).

The organic horizon at the Bean ring comprises peat and is described as per the organic layer at Thorn North. The uppermost clay in most areas at the Bean ring show mottling or an orange/red-dish colour due to oxidation and intermittent unsaturated conditions. This unit is referred to at the Bean ring as ‘mottled clay’ and sampled as a different horizon. Only the deeper clay data and peat data are discussed below. All samples from BE–SWNE and approximately two thirds of the samples from BE–SENE show some degree of oxidation. As a result of a deep, peat-filled depression in the mineral soil beginning at the ring edge, none of the clay samples within the ring on the SE axis showed any degree of oxidation. This is important in interpreting the soil geochemical data as discussed below.

The Bean ring, with a diameter of 430 m, is situated on a black spruce-dominated forest. A circular stand of black spruce surrounds the ring (Fig. 6) 75–100 m outside the light-coloured annulus and is referred to here as the ‘black spruce aureole’. Such aureoles are rare and have only been noted at a few other rings. Two orthogonal transects were established: BE–SWNE (SW–NE) and BE–SENE (SE–NW; Fig. 6). The surface is gently sloping to the west, with an overall relief of 5 m across the 1 km long BE–SENE transect.

Twenty-three shallow monitoring wells (Hamilton & Cranston 2000) were installed at 9 m depth within the glacial sediments (Fig. 7). Methane gas continually escapes as bubbles from groundwater and the well casings of the five central shallow boreholes (Fig. 7). In several of the central boreholes gas loudly hissed through the well screen when the water level was pumped down to below the top of the screen (*c.* 7.5 m depth). No gas has been observed or detected in groundwater from the central monitoring well drilled into rock (arrow, Fig. 7) but the drill-collar briefly ignited during drilling and before the overburden had been cased off. The rapidity by which gas enters the well screen suggests vapour-phase  $CH_4$  resides in the permeable sand lenses in the clayey tills. The hydraulic head in the monitoring wells is up to 2 m above ground surface, indicating artesian conditions across the

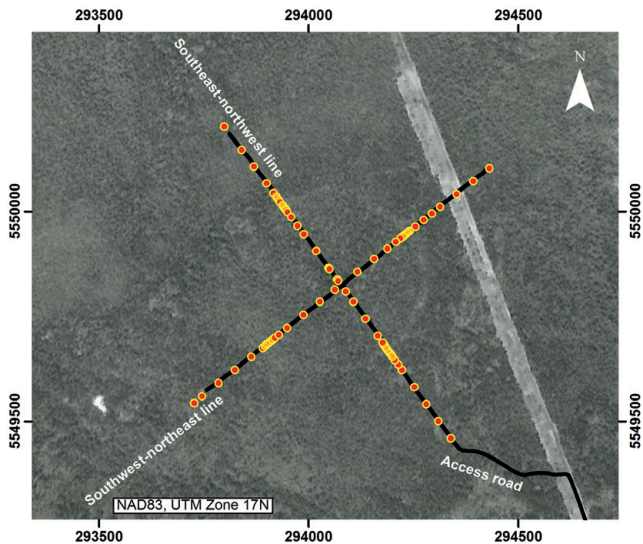


**Fig. 6.** The Bean ring (430 m in diameter) showing sampling transects of SE–NW (BE–SENW) and SW–NE (BE–SWNE). Sampled locations are shown as circles. Note the darker black spruce aureole surrounding the ring. Geo-positioning of the air photo is estimated to be accurate to  $\pm 10$  m but was rubber-sheeted to a Landsat image of unknown accuracy. The photo is clipped from an Ontario Ministry of Natural Resources air photo number 86-5003-09-62.

ring. Artesian conditions in the Quaternary sediments are more pronounced with increasing depth. Peat and soil are saturated across the ring for at least part of the year. The hydraulic head in bedrock at the centre of the site is almost 4 m above ground surface.

**Methodology**

**Sampling**

Soil and peat samples at the Bean ring were collected in August 1999 for a hydroxylamine-HCl leach and in July 2000 for an *aqua regia*

digestion. Samples at Thorn North were collected in July 2000 for *aqua regia* digestion. The same sampling methodology was used during both years. Samples for carbonate analysis were taken from splits of the *aqua regia* samples. Two orthogonal sampling transects were established across each ring (Figs 4 and 6). The sample spacing at the Bean ring was 50–100 m in 1999 and for both rings 25–50 m in 2000; the longer interval each year (100 and 50, respectively) was used far outside the ring to establish distal background conditions. For both years, a tighter sample interval of 5 m was used across each ring annulus.

During sampling, peat thickness was first assessed by measuring the depth to clay with a split soil spoon. One soil spoon length (30 cm) of mineral soil was collected beneath the peat–soil interface. Peat samples were collected within 30 cm of the clay sampling site, at the standard depth of 0.5 m using hand-held augers (Figs 5 and 7).

**Identification of ring edges**

This study seeks to study underlying causes for the visual expression of the Bean and Thorn North rings and therefore precise identification of the location of the ring edge is important. Although the edges are easily located from aircraft and on air photos, the edges are not apparent on the ground. The ring edge was determined by placing white markers along the transects, 10 m apart at each of the presumed ring edges and using oblique aerial photos taken orthogonal to the sampling transects to revise the position of the ring edges. At the Bean ring, the positions were revised again slightly using recent Google Earth® imagery that is detailed enough to identify both the ring edge and the sampling transects.

At the Bean ring (Table 1), the outer and inner ring edges were found to be between 18 and 30 m apart on the SE, NE and NW axes. These parts of the ring lie in black spruce forest. The SW, located in a tamarack and cedar swamp, is more difficult to define. The inner edge is more clearly defined and was thus used to estimate the position of the outer edge by assuming a 20-m width to the ring on that axis. The error on the location of the centre of the

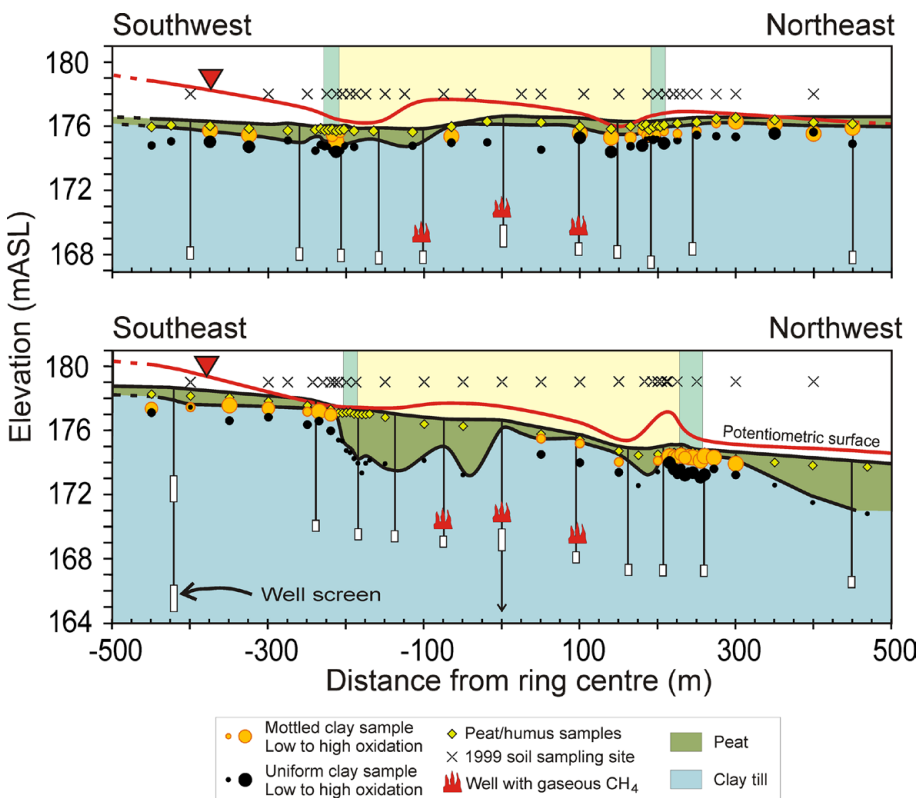


**Fig. 7.** Stratigraphy, well and soil sample locations at the Bean Ring SW–NE and SE to NW sampling transects. The thick vertical green bars indicate the position of the ring edges. Methane is present in vapour phase at flammable concentrations in the five central wells (the central shallow borehole is shown on both transects) but not in the deep borehole, shown as an arrow in the bottom figure. The visually estimated degree of oxidation is shown as increasing circle size. Note the decreased degree of oxidation inside the ring on the SE axis. Samples collected in 1999 (i.e. weak leach samples) were clay samples collected directly at the interface of peat and clay without distinguishing the different clay horizons. Note the large vertical exaggeration.

ring edges is estimated to be  $\pm 10$  m except on the SW transect, where it is likely 50% poorer ( $\pm 15$  m).

At Thorn North (Table 1), the inner edges were clear and a consistent distance from the outer edge. On the north, south, west, and SW edges, the position is estimated to be accurate to  $\pm 5$  m, and on the east and NE edges to  $\pm 10$  m. The large uncertainty on the eastern side is due to a change in vegetation over the north–south-trending esker that underlies the eastern third of the ring. Where the inner edge is visible, it is between 15 and 20 m from the outer edge.

### Field analyses

Peat pH and ORP measurements were made within 24 hours of sampling. Wet peat was placed in a cup and compressed to release trapped air bubbles and to squeeze out contained water. Clay samples were mixed into a slurry with deionized water (1:1 mix by volume) prior to measurements.

The pH probe was a glass-bulb, gel-filled Corning Ag/AgCl combination electrode. It was three-point calibrated at pH 4, 7 and 10 at the beginning of each day, cleaned with deionized water after each measurement and stored between samples in a pH 7 buffer solution. The ORP probe was a commercial Ag–Ag/Cl combination electrode (Corning model 476516) and, as is typical with platinum ORP probes, was not calibrated. The ORP readings followed methods presented in Hamilton *et al.* (2004b). ORP is the voltage difference between the half cell and the platinum electrode in contact with the sample as measured using a very high impedance voltmeter (usually a pH meter in mV mode). Under ideal conditions, the voltage reading is proportional to the redox difference between the half-cell and the solution in contact with the Pt electrode. To minimize the effects of polarization, the probe was dipped (*c.* 1 s) in a reducing pre-treatment solution (acidic ferrous-sulphate; Hanna Catalogue No. 1230) and immediately rinsed with distilled water prior to each new measurement. To allow for further depolarization, ORP values were recorded after 1, 2 and 5 minutes of immersion in the solution. ORP readings typically followed a continuous trend (decrease or increase) during this period of time but to wait for complete stabilization would have led to unreasonably long measurement times. In all cases, the reading 5 minutes after the immersion was used as the representative value. Between samples, the probe was cleaned with distilled water and kept in the recommended KCl storage solution, which has the same molarity as the filling solution, in order to minimize contact with air. When resuming measurements after a storage period longer than 2 hours, the first sample slurry was repeated: the first time to depolarize, and second to obtain a lower, depolarized and more accurate reading for that sample. To avoid loss of consistent data in the event of a failure of the (uncalibrated) ORP probe, two probes were used simultaneously, and therefore all slurries were measured a total of 6 times. The data-set for the ORP probe that showed the highest relief was used herein. pH measurements were made with one probe in triplicate at 1, 2 and 5 minutes and there was much less of a difference between the readings than for the temporal ORP data. The 5-minute pH dataset is used herein.

### Laboratory analyses

Peat and clay samples were oven dried at temperatures below 60°C, gently disaggregated using a ceramic mortar and pestle and sieved to –230 mesh (ASTM; <0.062 mm). The mineral-soil and peat samples collected in 2000 were digested with *aqua regia* and analysed using inductively coupled plasma mass spectrometry (ICP-MS) and inductively coupled plasma optical emission spectrometry (ICP-OES) at the OGS Geoscience Laboratories (Sudbury, Ontario, Canada). Total carbonate content was determined on split samples using the Chittick method, which measures the volume of CO<sub>2</sub> released from a finely ground sediment sample

after adding hydrochloric acid (Dreimanis 1962). The Chittick methodology also determines the calcite and dolomite content based on the different rate that calcite and dolomite evolve CO<sub>2</sub> with the addition of acid.

Soil samples collected in 1999 were split. One half was subjected to a hot hydroxylamine-HCl (0.25 M NH<sub>2</sub>OH·HCl at 60°C) leach after the method of Hall *et al.* (1996) by Activation Laboratories, Ltd. (Ancaster, Ontario, Canada) and the leach solution was analysed by ICP-MS. This method was used because it selectively leaches amorphous iron oxides and any co-precipitating and sorbed phases. The second split was analysed following *aqua regia* digestion by ICP-MS at the OGS Geoscience Laboratories.

Approximately 5% of the samples collected in the field were duplicate pairs. The precision of the carbonate analysis using the Chittick method based on field duplicate samples is 8.7% for dolomite content and 10.3% for calcite. The determination of cations gave the precision of 8.3% for Fe, 0.09% for Mn, 16.0% for Al, 13.9% for Mg, 20.1% for Ca, 22.2% for Mg, 18.8% for S, 16.6% for Ti, and 17.2% for Zr.

### Principal Component Analysis (PCA)

The PCA was carried out in the R Programming Environment. The program extracts the components through the principal axis method followed by an orthogonal rotation. This is a simple rotation of the data in multidimensional space that maximizes the sum of the variances of the squared loadings without actually changing the relative (multidimensional) spatial relationships between samples. The procedure is not iterative and calculates a unique solution.

### Data analysis

Prior to input, the data were tested for normality using Q–Q plots and not transformed. Standardization was automatically applied to the variables by the software. The PCA test was performed on selected data from the *aqua regia* and Cal, Dol, pH and ORP for the mineral soil samples on transects at the Bean ring because it had the more consistent sample media. Ten variables were included in the PCA: calcite content (Cal), dolomite content (Dol), ORP, pH, and concentrations of Fe, Mg, Mn, S, Ca, and Zr.

Extremely high correlations in the lithophile elements occur in this data-set because of inconsistent weathering in these high carbonate, immature soils. The fairly uniform, exotic, clay till parent material has a typical carbonate content of 40% but can vary in the mineral soil samples between 4.3% and 52%. This concentrates the siliclastic component and all the lithophile elements in tandem and creates high correlations. Because the ring-edge processes may be obscured by the effect of weathering processes, it was essential to limit the number of these high correlating elements in the PCA. Therefore a large number of elements were not included despite being available through analytical results. These included a group of largely lithophile elements that displayed >0.99 correlations: Al, K, Ti, V, Ba, Zn, Co, Cr, Cs, Cu, Ga, Li, Lu, Pb, Rb, Th, Tl, Y, and REE. These elements were excluded to reduce the amount of variance redundancy within the data-set. Zirconium was kept as a proxy for these elements, as it displayed a correlation of >0.99 with almost all of the excluded elements but correlates more poorly with Fe (<0.99).

The data from both sampling transects at the Bean ring were combined and input as one population, resulting in a sample size of  $n=73$  (39 sites along SENW, and 34 sites along SWNE). The distinction between SENW and SWNE is not expected to skew the PCA because the sampling media on both transects are similar, as indicated by similar siliclastic and carbonate contents. For statistically reliable results, the minimal number of samples should be

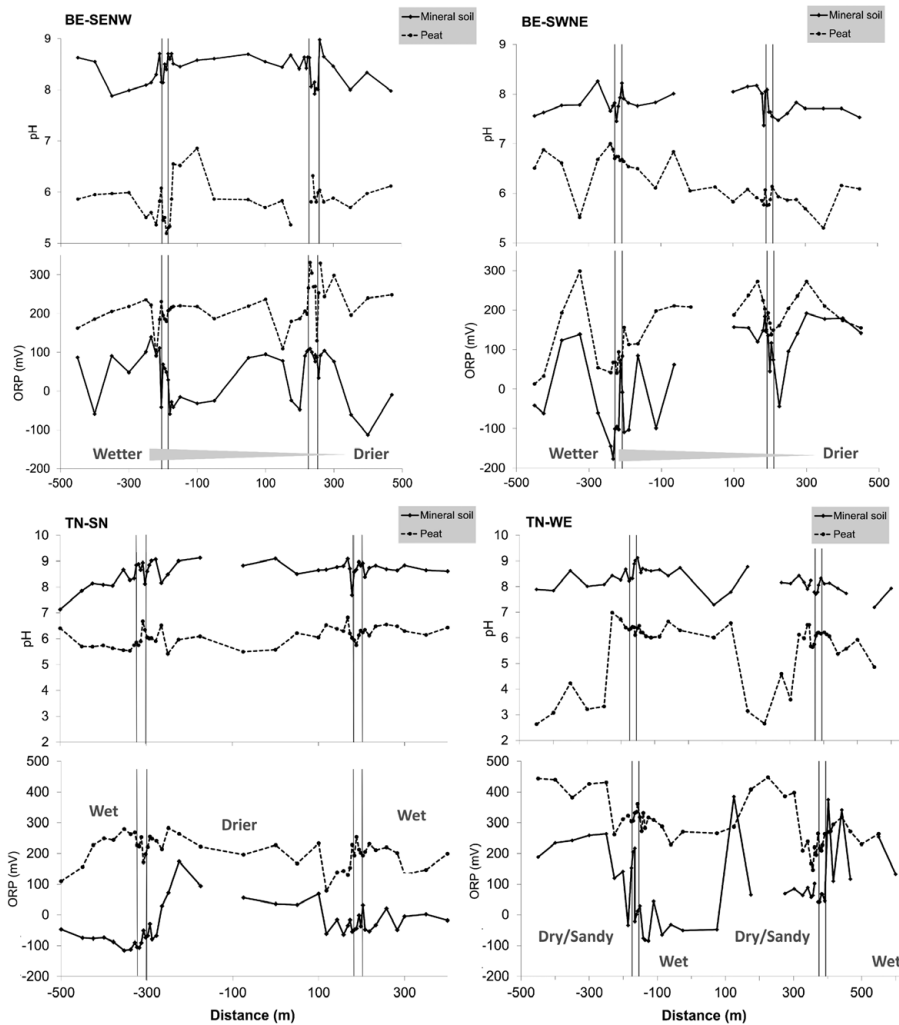


**Fig. 8.** pH and ORP variation of peat and mineral soil slurries along transects across Bean and Thorn North rings.

greater than 5 times the variables analysed (SAS Institute Inc. 2012). For this analysis,  $n/p = 10/73$  and therefore this precondition is achieved. The validity of the observed trends is also justified by their close geographical association with the ring edge, by comparison with line plots of the input parameters and by the geological significance of the assemblages of elements extracted in the principal components, as discussed below.

## Results

### Geochemical trends along transects

#### pH and redox

At the two rings, the pH of clay slurries ranges between 7.5 and 9.2, whereas the pH of peat samples ranges between 2.5 and 7.0 (Fig. 8). Peat along the TN-WE transect gives low pH values ranging from 2.5 to 4.5 on the westernmost 5 samples and a block of 4 in the centre of the ring. Low pH values are spatially correlated with low moisture content at these sites and a change from well humified moist peat (high pH, low ORP) to poorly saturated humus samples (low pH, high ORP). This coincides with the occurrence of oxidized sand in the mineral soil at the first 5 sites along the transect and partially oxidized clay in the 4 samples near the centre. In addition, the water table drops at these sites.

The six ring edges of the BE-SENW, BE-SWNE and TN-SN transects are characterized by distinctly low pH of clay slurries. The observation could not be made on the TN-WE transect because of variable media on that line. At these six ring edges, and particularly on the BE-SENW and TN-SN transects, the drops in

pH are framed by distinctly high pH areas that are 50–100 m wide. There is no pH high on the outer northeast edge at Bean ring, but here the sample density does not appear to adequately cover the area. At the Bean ring, from the adjacent peaks to the pH lows at the centre of each ring edge, the drop in the clay slurries averages 0.81 pH units. At TN-SN a drop in pH between the adjacent peaks and the ring edge averages 1.2 pH units.

The pH of peat is more variable than that of the clay slurries. Spatial variations at the ring edge are characterized by sharp increases rather than decreases and these changes occur above or almost above the pH lows in clay. Positive values in peat pH at ring edges are most evident at BE-SENW, BE-NE and have adjacent lows on either side. The magnitude of the peaks, as measured from the adjacent troughs, average 0.8 pH units at Bean and 1.0 pH units on TN-SN. It is unclear whether the peak at BE-SW is missing, or is wider and less sharp. The antithetic mineral soil/peat pH relationship is offset by one sample station at both ring edges on the TN-NS transect. This may be a result of a slight misalignment of the peat and clay samples because sample stations were spaced very close together and samplers could never collect peat from exactly the same location as the clay sample. This was to avoid siliciclastic contamination from the sampling of the clay, which was always collected first.

#### Oxidation-reduction potential

Shallow peat samples have higher ORP values and greater variability than deeper clay samples (Fig. 8). The measured redox state of the peat correlates with moisture content with water-logged anoxic peat being more reduced. Oxidized, dry and sandy samples

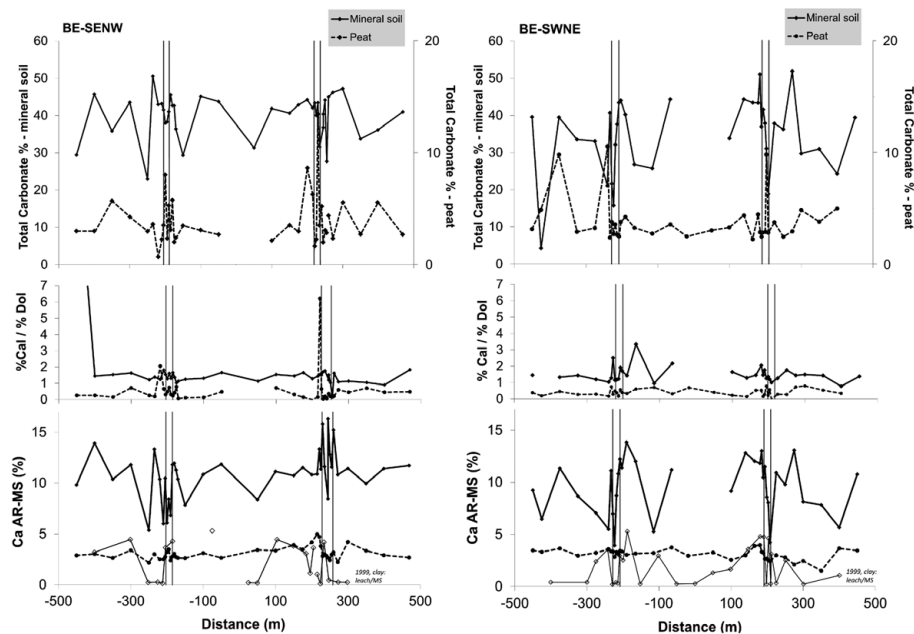


**Fig. 9.** Contents of carbonate, calcite, dolomite and Ca in peat and mineral soil at Bean ring. Note that sampling sites and sample depths vary slightly between 1999 and 2000 studies (as indicated in Fig. 7).

alternate with reduced, wet and clay-rich samples along TN–WE transect (Fig. 8).

Clear spatial variation of ORP in both peat and mineral soil occurs on all ring edges except for TN–SN. The variability of ORP is greater than pH, and large amplitude changes coincide with pH lows in clay at ring edges. This is evident at BE–SENW, where pH lows in clay on the outer side of the ring edges are coincident with large dips in ORP with amplitudes of 150–200 mV in the peat and 50–150 mV in the clay. Responses on BE–SWNE also show large amplitude changes but since the sample density was not perfectly optimized for the ring edges, the pattern is not as clear. Changes in these parameters in peat and mineral soil are offset by several sites, but ring edges in wet conditions along the NE transect appear to correlate a low in the pH/ORP of clay with a low in the ORP of peat, whereas dry ring edges along NW and NE transects correlate a high in the ORP of peat with a low in the pH/ORP of clay. By and large across the Bean ring, the ORP in clay is low inside the ring on the BE–SWNE transect and mostly low also inside the ring on the BE–SENW transect. The exceptions are three samples inside the ring on the NW side. These are in an area of particularly shallow peat where the clay is partially oxidized.

A wide and more oxidized zone occurs inside of the ring edges at TN–SN transect in mineral soil, but not within peat. The clay in this area appears unoxidized and the trends in other parameters (pH, Ca, total carbonate, major elements; see below) do not show this response. The gap in the sampling at –110 m on the TN–SN transect was due to the presence of oxidized sand and no clay. This positive response may be related to a drastic drop in the potentiometric surface in the underlying clays in this area (Fig. 5), perhaps due to under-drainage into the esker. This could allow periodically unsaturated and oxidizing conditions in the clay and overlying sand. Hamilton & Hattori (2008) noted reduced conditions in the groundwater in this area, suggesting the oxidized upper clay is likely a shallow phenomenon.

#### Carbonate content

The changes in sample media on the TN–WE transect and particularly at the east edge render interpretation difficult and the data are not discussed. However, the other transects at both sites show a relationship between Ca content and carbonate content (Figs 9 and 10). The mineral soil is characterized by low total carbonate and

by *aqua regia* Ca (Figs 9 and 10). Although different sampling stations were used at the Bean ring for the samples collected in 1999, it shows a similar drop in Ca in approximately the same ring edge locations as the drops in carbonate and *aqua regia* Ca. In mineral soil at the Bean ring, the calcite/dolomite ratio shows a minor decrease at the ring edge with flanking highs on both sides but the Thorn North ring shows no apparent change.

The change in carbonate content in peat is antithetic to that in the underlying clay. Where carbonate content drops in mineral soil, it rises in peat, usually several-fold and manifests as sharp peaks on either or both sides of the ring edges. This affects the calcite/dolomite ratio (cal/dol) in peat, which shows sharp increases at some ring edges. The change in carbonate content in peat at the ring edge is underscored by its symmetry and position relative to the responses in mineral soil.

The changes in carbonate content in peat are generally reflected in changes in Ca concentration, although this is more apparent at Bean ring than the Thorn North ring.

#### Elemental abundance

Soils at both the Bean and Thorn North sites are immature with incomplete or no soil horizon development. The high carbonate content of the parent clay and the variable amount of weathering-related carbonate removal result in a highly variable siliciclastic component in the soil residual. Since ring edge processes are postulated to include numerous redox-sensitive elements that are also affected by these weathering processes, it is necessary to reduce the variability in the data-set that results from strictly soil processes. To achieve this, contents of Fe, Mn and Al by *aqua regia* digestion of peat and soil samples are normalized with Ti in order to minimize the effect of variable siliciclastic component in the soil residual (Fig. 11, Bean; Fig. 12, Thorn North). This greatly enhances the ring-edge variability for these elements and smooths variability elsewhere along the transects. The ratios of Fe, Mn and Al to Ti in *aqua regia* digestion of clay show higher values on the dry ring edges (BE–NE and BE–NW) than the wet ring edges (both edges on TN–SN; BE–SW and BE–SE). Iron and Mn, which are redox-sensitive in soil, have similar patterns although the patterns for manganese are more subtle. Aluminum shows a different pattern and is not redox active but its solubility is strongly influenced by soil pH. The occurrence of the peaks and lows in Fe and Mn abundances in clay coincide with the locations of the pH lows



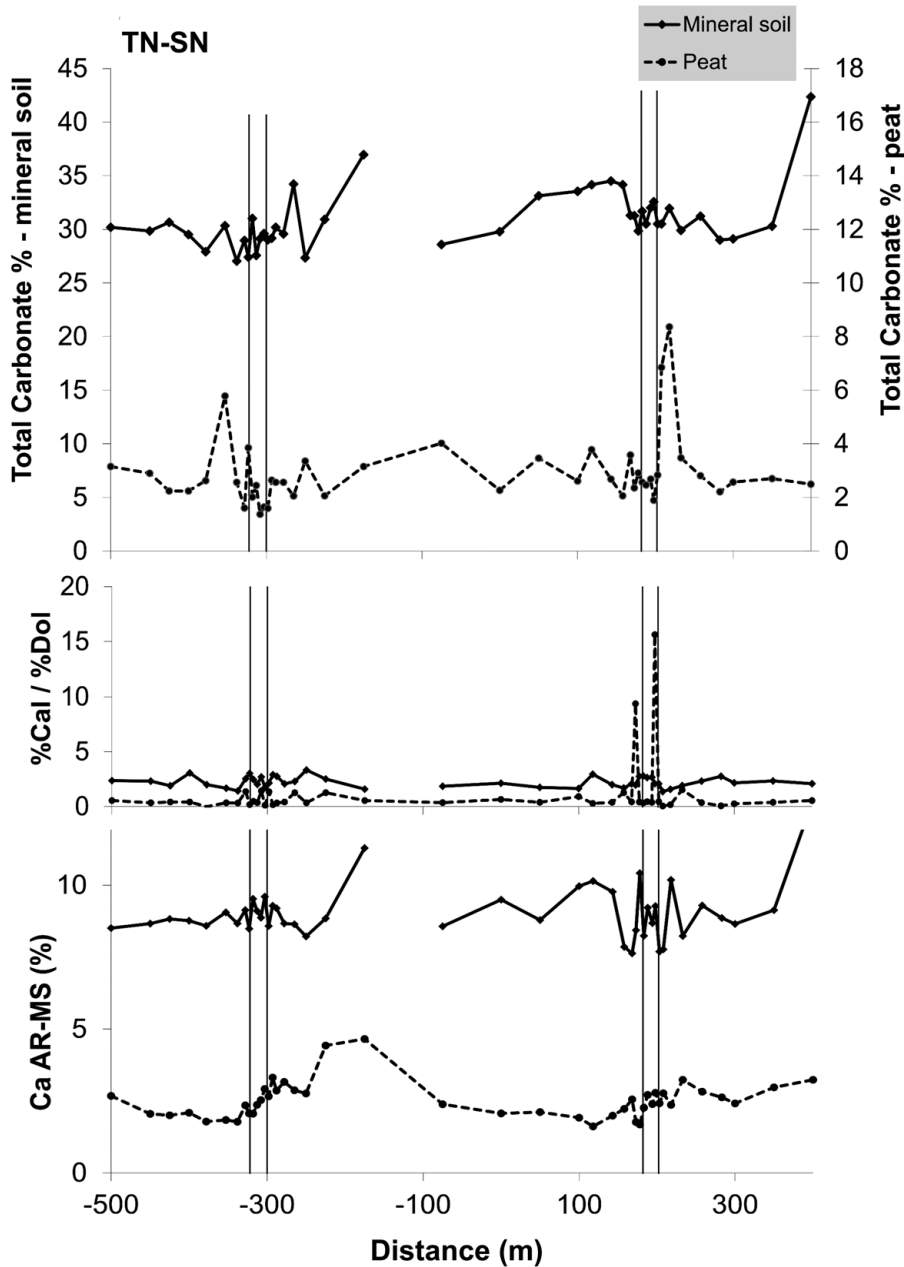


**Fig. 10.** Carbonate content and proxies in the organic and mineral horizons at Thorn North on the TN-SN transect (the TN-WE transect exhibits strong variability due to changes in the sampling medium). As with the Bean ring, positive carbonate responses related to the ring edge are apparent in the peat samples and in particular on the north, south and western edges. Weak leach data were not collected at Thorn North.

and carbonate depletions. Thus, they also correspond to the sharp ORP lows at the ring edges. Titanium-normalized Fe and Mn in peat exhibit higher ratios where lower ratios were observed in the underlying clay, that is, in wetter peat on the TN-SN transect and on the southern two ring edges at the Bean ring. The higher ratios in Fe at both edges of the TN-SN transect, and for Mn on the north edge, are surrounded by broad enrichments up to 200 m wide that are centred on each ring edge. Antithetic metal responses in peat and clay on all six ring edges suggest that clay is the likely source for the metals in the peat.

The hydroxylamine-HCl leach is considered to dissolve amorphous Fe oxides and Mn-oxides and as such, it is a weaker leach than *aqua regia* digestion (Hall *et al.* 1996). The data for the hydroxylamine-HCl leach for Fe and Mn in the mineral soil normalized, respectively, against Fe and Mn by *aqua regia* enhance a signal for the mobile component of metals. The results at the Bean ring (Fig. 11) show lower concentrations of Fe and Mn across the ring relative to the outside, presumably because there are fewer amorphous Fe oxides in the reducing environment within the ring. There are significant highs in Fe and Mn by the hydroxylamine

leach at the ring edges, even on the wet edges where metals in *aqua regia* show low concentrations. This suggests that soil and peat at the ring edges maintain mobile metal components. On the wet ring edges, metals are weakly adsorbed on amorphous Fe- and Mn-oxides without converting into more crystalline phases.

### Principal Component Analysis at the Bean ring

#### Principal component loadings and interpretation

The PCA yielded 10 components, the first 2 of which explain close to 60% of the variability. The proportions of the variance they accounted for are, respectively, 42% and 17%. The remaining components are of minor importance, accounting for 12, 8, 6, 6, 3, 2 and <1% of the variance and are not discussed here.

PC1 (Fig. 13) has strong positive loadings, in decreasing order, for calcite (Cal, 0.43), Ca (0.34), S (0.32), and dolomite (DoI, 0.26); and strong negative loadings, in decreasing absolute values for Fe (-0.44), Zr (-0.36) and Mn (-0.35). ORP, pH and Mg all display minor positive loadings. PC1 represents elements related to carbonate, or the inverse of a siliciclastic component,

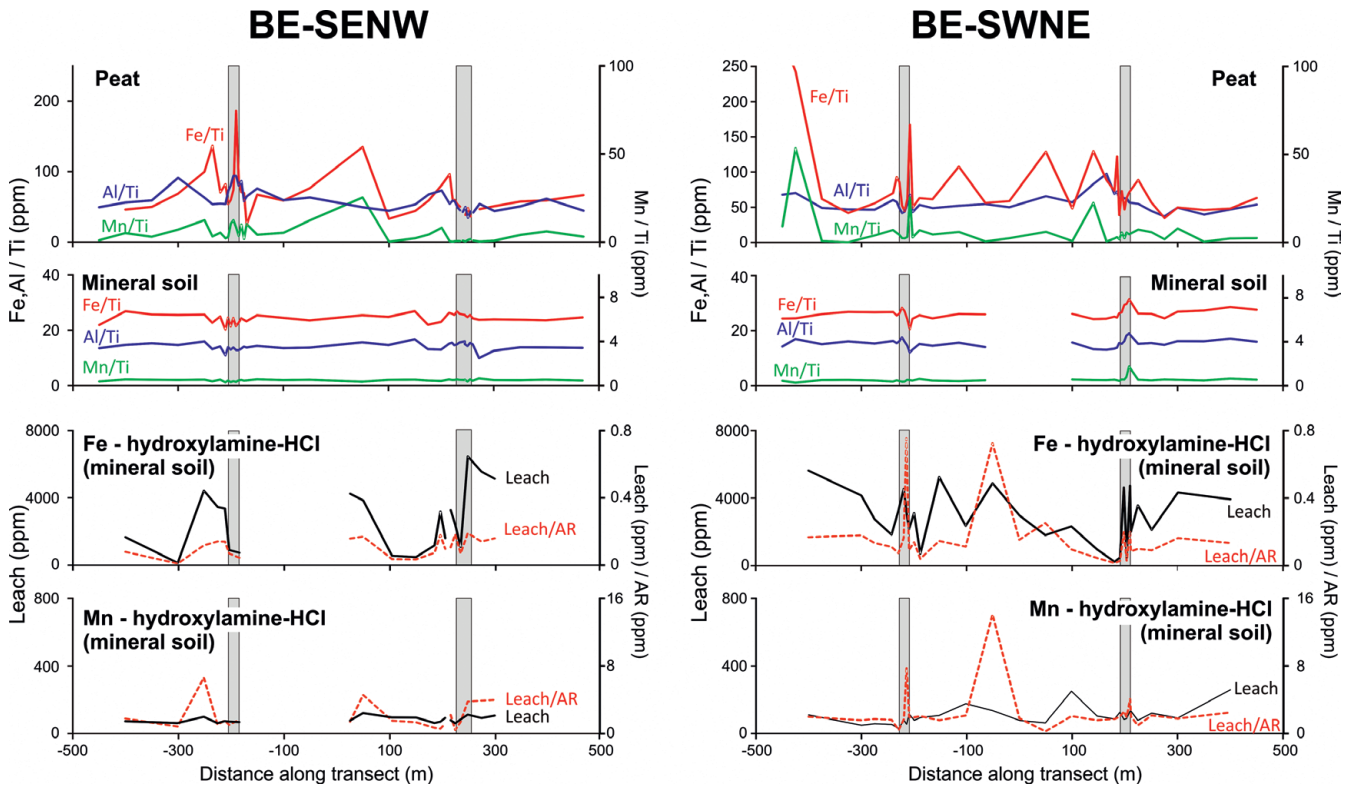


**Fig. 11.** Soil geochemical data for peat and mineral soil at the Bean ring. Fe/Ti, Mn/Ti and Al/Ti ratios by *aqua regia* from the 2000 sampling are shown; Fe and Mn data by hydroxylamine-HCl and *aqua regia* are shown for the 1999 sampling. Note that sampling sites and sample depths varied slightly between the hydroxylamine-HCl and *aqua regia* sampling (as shown on Fig. 7).

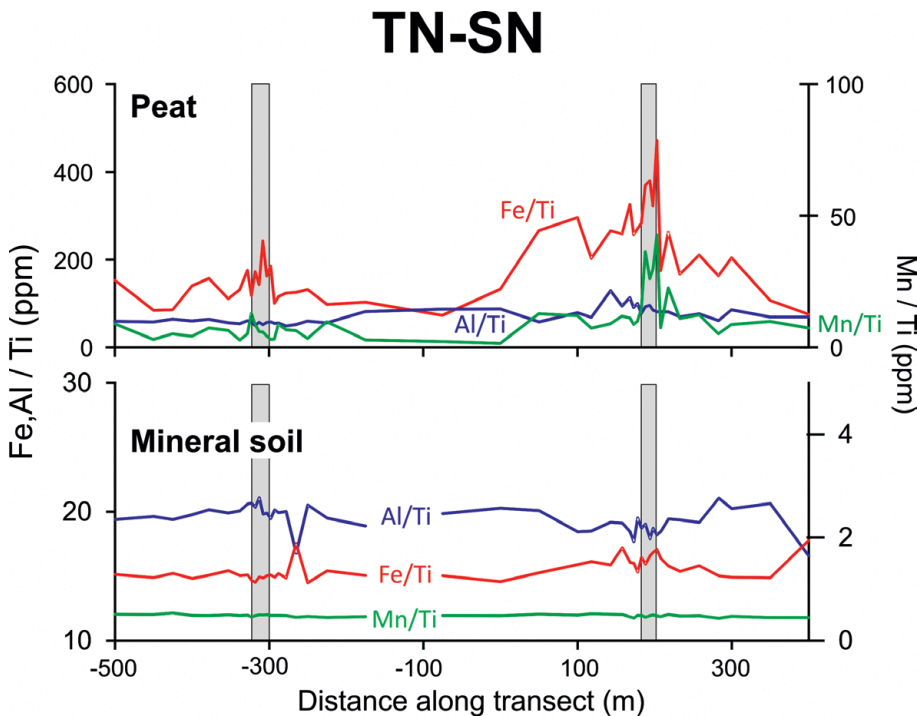


**Fig. 12.** Soil geochemical data for peat and mineral soil at Thorn North. Fe/Ti and Mn/Ti ratios by *aqua regia* are shown only for the TN-SN line; sample media were too variable on the TN-WE line to allow interpretation.

i.e. the negatively loading elements would remain unchanged in mass but increase/decrease in concentration during the removal/addition of carbonate, which is represented by the positive-loading elements. PC2 is dominated by variables related to dolomite, which load, in decreasing order Mg (0.66), Zr (0.37), Ca (0.31), S (0.3), Dol (0.26), and negatively loads pH (-0.33). Iron, Mn and ORP have weak positive loadings and Cal has almost no loading. Scores of PC2 are high at the outer ring edges (Fig. 13),

demonstrating an inverse correlation between pH and dolomite in these sites.

*Principal component scores in the identification of edge-related responses*

Figure 13 displays the PC scores of variables along the transects at the Bean ring. Scores for samples collected below 2 m of peat are marked as white squares (Fig. 13). The SE ring edge is excluded

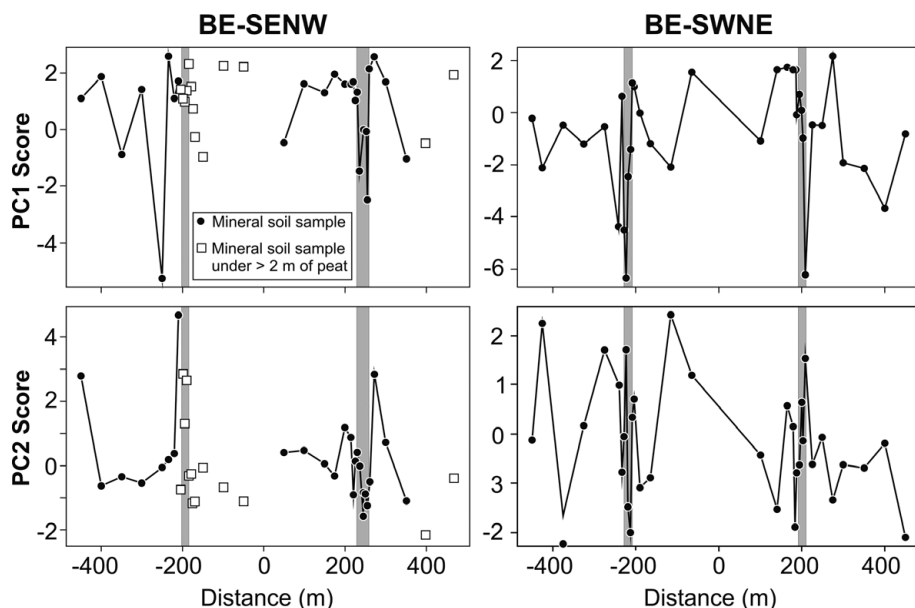


Fig. 13. Principal component (PC) scores across the two transects at the Bean ring.

from the discussion because of the change in the medium due to the deep peat-filled topographic depression just inside the ring edge. The three ring edges show evidence for chemical reactions and display very prominent twin-peak highs in the scores of both principal components, although the position of these twin-peak highs relative to the ring-edge differs slightly. PC1 shows lows in the outer ring edge with adjacent highs that are 50–75 m across, and PC2 shows lows that are biased toward the inner ring edge with sharp highs just outside the ring edges.

The antipathy in PC1 between  $Ca/Cal$  and  $Fe/Zr/Mn$  indicates that calcite removal (or addition) results in concentration (or dilution) of the siliciclastic component and that the degrees of antipathy are greatest in the ring edges. This antipathy is attributed to an addition of  $Fe/Mn$  and simultaneous dissolution of calcite. The most profound lows in PC1 (carbonate/residual) coincide with highs in PC2 (dolomite) at the outer ring edges on BE–SENW. They occur where the calcite/dolomite ratio is lowest (Fig. 9). Considering pH has negative scores in PC2, the relationship between PC1 and PC2 suggests that dolomite is being concentrated in soils at the outer ring edge during the removal of calcite by acidification. This proposed interpretation is supported by high positive loadings for Zr in PC2.

## Discussion

### *Synthesis of geochemical responses at the ring edge*

Ring edges show co-variations of many geochemical parameters including redox, pH and carbonate content within a short distance. These changes show a twin-peak pattern over the ring edge. The PCA confirms that the elements with the strongest responses at the edges of BE–SWNE and the NW axis are Fe, Mn, pH, ORP, S, Ca, Mg, Cal for major parameters, and for Zr as an indicator of the soil residual component.

The edges of both rings show characteristic patterns (Fig. 14). In particular, a sharp, narrow dip in pH, typically of 1–2 sample stations across 5–10 m, occurs on all ring edges, despite the visible ring edge being typically 20 m in width. The edge-related geochemical processes are more widespread, extending up to 75 m from the ring edge on both sides, and include elevated carbonate content in the mineral soil. At the Bean ring, these areas approximately correspond with the visible black spruce aureole. This aureole is a zone of more robust forest growth that has an important spatial relationship with the ring. It may result from an increase in

the bioavailable nutrients as a result of the presence of the reduced chimney.

At the ring, edge carbonate and pH show almost completely opposite patterns in peat versus mineral soil. The peat is characterized by positive pH responses, whereas the clay shows pH dips. Carbonate enrichments in the peat occur either directly above depletions in the clay or are offset slightly, usually outward.

Since PC1 is related to calcite, it shows the effects of variable soil acidity, which partly result from oxidative weathering of soils. However, it clearly indicates acidic conditions in the ring edges (negative loading of Cal, Ca, Dol, and pH) where ORP is lowest, therefore indicating reduced conditions where acid is being generated. Zirconium is almost immobile in aqueous solutions at low temperatures and it is used as a proxy for the siliciclastic component. It loads strongly negatively in PC1 and strongly positively in PC2. Lows in PC1 in the inner annulus on BE–SWNE suggest that removal of carbonate and volume reduction results in a higher siliciclastic component. Highs in PC2 in the outer annulus of BE–SWNE suggest siliciclastics and dolomite are also concentrated on the outer ring edge. The PCA analysis therefore supports consumption of all carbonate in the inner annulus and preferential consumption of calcite on the outer annulus, thereby concentrating dolomite. This supports the calcite/dolomite ratios which show lows in the outer ring annulus at the Bean ring.

The transect data additionally show that edges are characterized by increases in oxidized products, as exemplified by the peaks in the concentrations of Fe and Mn that occur at almost exactly the same location as the ORP dips.

### *Proposed reactions at the ring edge*

The spatial variation observed at ring edges is similar to that observed above reduced chimneys associated with buried metallic mineral deposits (Hamilton & Hattori 2008). It has been proposed (Hamilton 1998; Cameron *et al.* 2004; Hamilton & Govett 2010) that reduced chimneys induce upward transport of reduced species, their oxidation, acid formation and subsequent carbonate dissolution. This model, based on soil geochemical studies over mineral deposits, predicts low Eh in the chimney and very strong, positive-outward, redox gradients at edges, decreasing pH, depletion in carbonate, increased  $pCO_{2(aq)}$  towards the edges and increased deposition of metal oxyhydroxides in soil.

The three ring edges at the Bean ring and the two at Thorn North with consistent media show similar geochemical patterns in these

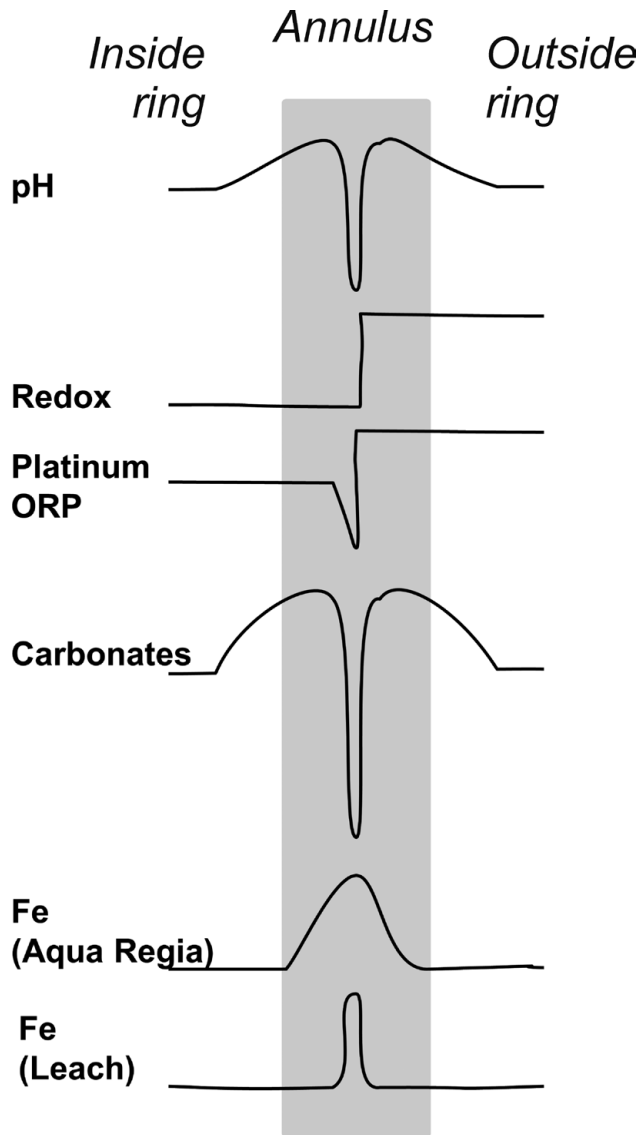


**Fig. 14.** Idealized responses within clay mineral soil in measured parameters at the ring edge.

**Table 1.** Location of ring edges (annulus), as determined from air photo interpretation, in metres with respect to the central well at each site. The central well is located where the two transects at each site cross

	Axis	Inner rim	Outer rim	Width of ring edge
Bean	SE	-185	-203	18
	NW	228.6	258.3	29.7
	SW	-208.2	-228.2	20
	NE	191.1	210	18.9
Thorn North	S	-322	-300	22
	N	202	182	20
	W	-174	-154	20
	E	394	374	20

parameters and support the proposed model. However, some observations are not explained by the model:

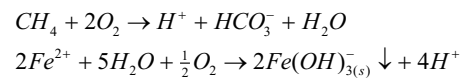
1. A coincidence of sharp ORP lows with the pH dips at the ring edges - this contradicts the model, which stipulated that pH changes occur in response to sudden increases in Eh at ring edges.
2. The antithetic response in pH and carbonate concentrations in clay and overlying peat.

The sharp drop in ORP is discussed in the next section. The remainder of the ring-edge processes are summarized in 5 stages (Fig. 15).

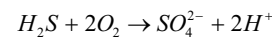
*Stage 1: Migration of reduced species from inside of the ring to the annulus.* The presence of  $\text{CH}_4$  at the Bean Ring and  $\text{H}_2\text{S}$  at Thorn North maintains redox-sensitive species in reduced form, including  $\text{Fe}^{2+}$  and  $\text{HS}^-$ . The gases and reduced ions disperse from high to low concentration outward to the ring edge. Reduced ions also migrate by electrochemical transport (Hamilton & Hattori 2008). Once reduced species are oxidized they are attenuated in a number of reactions that further promote dispersion. For example, deposition of metals maintains activity gradients at the ring edges and promotes their diffusion. At the Bean ring, artesian conditions of groundwater may possibly contribute to the upward transport of metals.

*Stage 2: Oxidation of species and acid production in annulus.* Oxidation of a number of species at the ring edge produces low pH conditions. At the Bean ring,  $\text{CH}_4$  and  $\text{Fe}^{2+}$  in groundwater are oxidized to form  $\text{HCO}_3^-$ , and  $\text{H}^+$  and precipitated  $\text{Fe}^{\text{III}}\text{O-OH}$ . At Thorn North, oxidation of  $\text{H}_2\text{S}$  produces sulphuric acid.

#### At Bean Ring

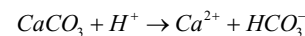


#### At Thorn North



At the Bean ring, the elevated Fe concentrations in clay indicate oxidation of  $\text{Fe}^{2+}$  to  $\text{Fe}^{3+}$ . The positive spikes in the ratio of Fe by weak leach v. *aqua regia* in the ring edge suggest active production of Fe oxy-hydroxides. The presence of localized low pH values at the ring edge is evidence for oxidation, including the likely oxidation of  $\text{CH}_4$  to form  $\text{CO}_2$  which would not leave direct chemical evidence in soils. Groundwater geochemical data at the Thorn North ring (Hamilton & Hattori 2008) indicate that the predominant reaction is oxidation of  $\text{H}_2\text{S}$  (as  $\text{HS}^-_{(\text{aq})}$ ) resulting in elevated  $\text{SO}_4^{2-}_{(\text{aq})}$ , particularly at the ring edges. Lows in soil-slurry pH and the changes in groundwater chemistry at the ring edges suggest  $\text{H}_2\text{S}$  oxidation in soils to form  $\text{SO}_4^{2-}$ , which does not leave direct evidence of the reaction because it does not precipitate as sulphate minerals in low Ca environments. Instead, it enters groundwater as  $\text{H}_2\text{SO}_4^{2-}_{(\text{aq})}$  and creates acidic conditions. Metal oxidation here is unlikely because most metals are insoluble in the presence of  $\text{H}_2\text{S}$ .

*Stage 3: Acid dissolution of carbonate in mineral soils at the annulus.* The formation of acid in the ring edge results in carbonate dissolution:



This interpretation is supported by the spatial co-variation of carbonate content and pH in clays at the ring edge. The PCA supports the calcite/dolomite ratios and suggests preferential consumption of calcite, and the residual concentration of dolomite, in the outer annulus. The PCA and carbonate data suggest that more robust acidification is occurring in the inner part of the annulus with both calcite and dolomite being consumed with non-carbonate residual phases being concentrated.

*Stage 4: Lateral migration of DIC/Ca rich fluid in the clay; re-precipitation of carbonate.* The dissolution of carbonate produces high Ca, dissolved inorganic carbon (DIC) and  $\text{pCO}_2$  in pore

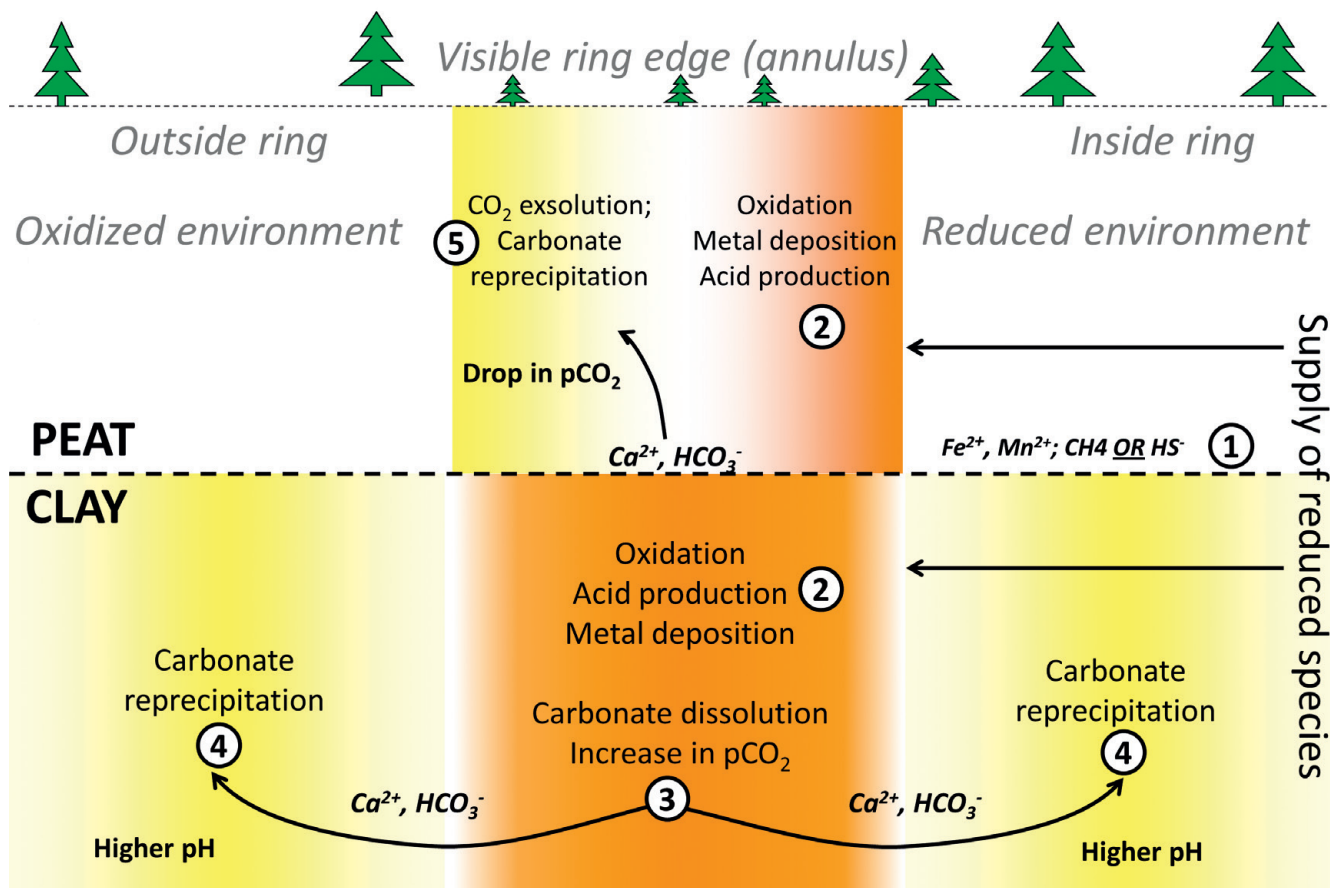
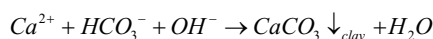
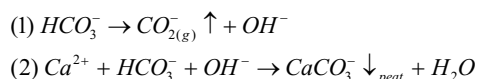


**Fig. 15.** Proposed model to account for spatial variation in redox and carbonate content at the ring edge. Numbers represent (1) migration of reduced species outward, (2) their oxidation resulting in acid production and deposition of metals, (3) acid dissolution of carbonate and the lateral dispersion of dissolved inorganic carbon phases and Ca, (4) re-deposition of carbonate in higher pH, marginal areas and (5) upward migration of DIC and Ca into peat followed by degassing of CO<sub>2</sub>, pH rise and deposition of carbonate into peat.

waters and promotes the diffusion of species ( $Ca$ ,  $HCO_3^-$ ) from the ring edge into adjacent areas. This lateral migration of carbonate-rich fluids explains high contents of  $CaCO_3$  in shallow soil flanking the pH lows in the annulus. Deposition of carbonate is a result of the more elevated pH in the surrounding environment:



*Stage 5: Vertical migration of DIC/Ca rich fluid; CO<sub>2</sub> degassing; deposition of carbonate into peat.* DIC and Ca-rich fluids from the clay diffuse upward into peat where (1) CO<sub>2</sub> degasses from water, raising the pH and lowering the solubility carbonate of until (2)  $CaCO_3$  precipitates:



This mechanism is proposed to explain the antipathy between the pH lows in the annulus in clay and pH highs in the overlying peat and the elevated carbonate in peat in the ring edge. Carbonate contents in peat are otherwise low due to low pH in peat water.

Note that reduced species within the peat would also migrate toward the ring edge, by the same processes described in Stage 1, and their oxidation would also produce acidity, which could interfere with carbonate deposition. At least on the BE-SWNE transect, the data seem to indicate that deposition of Fe-Mn oxides occurs in peat at the inner edge of the annulus, whereas deposition of carbonate occurs at the outer edge. The shift in the oxidation front in peat toward the inner ring edge is explained by generally higher

oxidation state in the peat stratum than in the underlying clay causing a shift in the location of metal oxidation inward towards the source of reducing agents.

### *The potential role of microorganisms in ring edge processes*

At the ring edges at the Thorn North ring, sharp ORP lows in soils coincide with pH lows that likely reflect oxidation reactions. This is similar to the process at depth as shown in monitoring wells at the same site (Hamilton & Hattori 2008). In the headspace of monitoring wells, trace concentrations of CH<sub>4</sub> up to 150 ppm occur at the ring edges, against background values near zero (Fig. 2). This is spatially correlated with drops in headspace O<sub>2(g)</sub>, and respective increases/decreases in SO<sub>4(aq)</sub>/H<sub>2S(aq)</sub> in groundwater in the same monitoring wells.

Unlike the Bean ring, CH<sub>4</sub> was detected only at ring edges at Thorn North ring suggesting it is produced there. Methanogenesis is an anaerobic process resulting from the reduction of CO<sub>2</sub> by autotrophic organisms and occurs under conditions more reducing than those required for sulphate reduction. Sulphate reduction is commonly coupled with methane oxidation into CO<sub>2</sub> through an electron shuttle process directly linking a methanotrophic Archea with a sulphate-reducing bacterium (Konhauser 2007). Therefore, it is unexpected that CH<sub>4</sub> and H<sub>2</sub>S, the products of two terminal electron acceptors, could apparently coexist within groundwater at the Thorn North ring edges especially in an area where (aqueous) sulphide oxidation is known to be occurring.

Biotic sulphur-oxidation dominates over abiotic oxidation where oxygen concentrations are low (Konhauser 2007) and therefore increased activity by anaerobic sulphur-oxidizing bacteria at the ring edges is likely. High microbiological activity and biomass that would be associated with sulphide oxidation may support smaller communities of heterotrophic methanogens, thereby generating the trace concentrations of CH<sub>4</sub> observed at the ring edges.

Like the geochemical patterns recorded at the Thorn North and Bean ring edges, low ORP values are reported in soils over mineral deposits that occur in locations in the overlying soils where the evidence for oxidation is strongest (Hall *et al.* 2005; Hamilton 2007). Examples include a soil survey above the Cross Lake base metallic sulphide deposit using a similar Pt-electrode slurry technique as this study (Hamilton 2007). The deep data from drilling demonstrated the presence of a reduced chimney in the 30 m thick glaciolacustrine clay that overlies the deposit. Soil-slurry ORP data show that symmetrical zones of highly reduced shallow soils occur at the locations where oxidation reactions are occurring above the reduced chimney. These areas show pH lows, elevated metal concentrations and carbonate depletion. Plate-counts show that sulphur-reducing bacteria are elevated in shallow soils over mineralization in this area (Hall *et al.* 2005), despite the abundant evidence for oxidation reactions. The sharp redox lows spatially correlate with elevated soil hydrocarbons and this was inferred to be reflective of bacterial biomass (Hamilton 2007). This is the same phenomenon as is inferred to occur at Thorn North except in a less reduced part of the electron transfer chain. At Cross Lake, the high microbiological activity and biomass of metal-oxidizing autotrophic bacteria appears to support smaller communities of heterotrophic sulphur-reducing bacteria.

Low ORP values in soils above forest rings and mineral deposits commonly occur where the evidence for oxidation is strongest and we suggest two non-exclusive explanations for this paradox:

1. Locally low-Eh values may reflect increased bacterial activity or biomass. These occur at the edge of reduced chimneys where redox gradients are most favourable for autotrophic organisms.
2. This may be an analytical artifact because autotrophic organisms commonly colonize electrode surfaces (e.g. Parra & Lin 2009). This yields erroneous ORP values relative to the bulk inorganic oxidation potential of the soil slurry but, in this case, the result would still be reflective of an area of increased microbiological activity in soils.

### **Implications for mineral exploration**

Twin-peak (sometimes called a 'rabbit-ear' pattern) and halo patterns of geochemical responses in soils over buried mineral deposits have long been recognized by previous workers (e.g. Govett 1973; Yeager *et al.* 1998). It has also been recognized or interpreted that many buried mineral deposits are accompanied by reduced 'columns' or 'chimneys' in overlying regolith materials (Hamilton 1998; Hamilton *et al.* 2004*b, c*; Cameron *et al.* 2004; Klusman 2009; Hamilton & Govett 2010). The geochemical responses are due in part to the different pH and redox conditions in the regolith materials hosting the reduced chimney, but also due to the mobilization of elements from the mineral deposits (Hall *et al.* 2005; Hamilton & Govett 2010). Differentiating primary from secondary geochemical features is important in effective identification of buried mineral deposits. Not only are secondary responses potentially misleading, their patterns hold clues to the geochemical processes that release ore-related compounds and transport and deposit them into soils.

The Thorn North and Bean forest rings are centred on geological sources of negative redox charge, which result in large, flat

reduced chimneys in glacial sediments that have more than 10 times greater horizontal extent than vertical depth. The reduced sources are non-metallic and mineral deposits do not occur in the vicinity of either, and yet they are associated with geochemical patterns that are similar to those documented over known concealed, metallic mineralization. The twin-peak responses and/or decreases in pH and carbonate species at both sites, the accumulation of redox-sensitive metals at the edge of the Bean ring and in sulphur species at Thorn North ring (Fig. 2) all occur in the absence of an underlying metallic deposit. Mobile metal responses at Bean are particularly intriguing since almost all such responses discussed in the literature are attributed to the presence of mineralization. Therefore, forest rings, at least at these two sites, provide a good opportunity to study the geochemical and microbiological character of the reduced chimney and related secondary responses. The results can serve as a base upon which to compare studies over mineral deposits to help elucidate true mineralization-related responses from those caused by the reduced chimney and other related secondary processes.

The study of forest rings may also shed light on the production of soil hydrocarbons. Soil hydrocarbon methods such as SGH® and Gore Sorber® are used, or are being considered, for mineral exploration. The apparent involvement of microorganisms in reduced chimneys in general, and forest rings in particular, demonstrates that these sites would be appropriate areas to investigate the contribution of redox processes in generating soil hydrocarbon responses.

### **Summary and conclusions**

Near the edges of two forest rings, oxidation of reduced species results in the precipitation of Fe and Mn oxyhydroxides, production of acidic conditions and the dissolution of carbonates. This model is commonly used to explain the development of geochemical dispersion anomalies in glacial sediments above metallic mineral deposits. Redox/pH sensitive geochemical parameters in soils on transects across buried mineral deposits often yield spatial distribution patterns symmetrical with respect to the centre of the reduced chimney that are commonly referred to informally as 'rabbit-ear anomalies' (Govett 1973). This study indicates that physical and chemical changes at the edges of rings are the result of the presence of the reduced chimney and result in chemical patterns that in some cases are profoundly symmetrical about the centre of the rings.

Major geochemical changes in the clayey mineral soil at the ring edges are characterized by a sharp, narrow (5–10 m) decrease in pH between wide pH highs; that coincides with a central carbonate low and much wider carbonate highs that extend outward up to 75 m on either side of the visible ring edge. These support the hypothesis that carbonate is being removed at the ring edge due to acid production and re-precipitated both inside and outside the ring where the pH is higher. Principal components analysis and comparative plots of geochemical data for shallow clay samples show distinct assemblages of parameters that co-vary at the ring edges. They suggest that calcite is being dissolved on the outer annulus of the Bean ring, concentrating dolomite in the soil residual, and all carbonate is consumed on the inner ring edge. This suggests more robust acidification on the inner annulus that diminishes across the 10–15 m to the outer edge. A comparison of data from mineral soil samples with that of overlying peat suggests that fluids with elevated pCO<sub>2</sub> and Ca migrate upward from the zone of acidification followed by degassing of CO<sub>2</sub>, a rise in pH and deposition of secondary carbonate in the peat. This process appears to be steady state with fluxes of CO<sub>2</sub> and Ca balancing the acidification processes associated with humification of the peat because there is no apparent build-up of travertine or visible carbonates. Metals

also oxidize in the peat but the zone of oxidation, at least at the Bean ring, is inward from that in clay by several metres.

A 75 m-wide aureole of robust forest growth surrounds most of the ring, roughly coincides with the increases in carbonate and may result from an increase in bioavailable nutrients surrounding the reduced chimney. This aureole and the carbonate depletions/enrichments in the visible annulus are a testament to the very large amounts of mass transport that must have occurred, in the 8kA since clay deposition as a result of the chemical and electrochemical processes that form the ring.

This work suggests significant microbiological processes at the edges of forest rings and that the ring-edge is the site of increased microbiological activity or biomass. These forest rings have no underlying mineral deposit and therefore all of the geochemical patterns observed, and responses proposed, are analogous to 'secondary' geochemical processes that would occur over metallic mineral-deposits as a result of the presence of a reduced chimney. Comparison of these data with similar data over mineral deposits may help to elucidate true ore-related signals over mineral deposits and differentiate these from responses due strictly to changes in Eh, pH and carbonate content.

### Acknowledgements and Funding

This project was supported by the Ontario Geological Survey and was part of an MSc thesis project by Kerstin Brauner. Fieldwork was carried out by a team from the OGS that included Devin Cranston and Boris Iotzov, with follow-up work by the Brauner in 2008, with field assistance from Victoria Lee. We would like to thank Dave Heberlein and another anonymous reviewer for their excellent and comprehensive reviews that greatly improved this paper.

### References

- Adams, P. 1998. *Overview of Biogeochemical and Geochemical Exploration*. Unpublished company report, Noranda Inc, Toronto.
- Brauner, K.M. 2012. *Geochemistry of Forest Rings in Northern Ontario: Identification of Ring Edge Processes in Peat and Soil*. MSc thesis, University of Ottawa. <http://hdl.handle.net/10393/23205> [last accessed 20 September 2015].
- Brauner, K., Hamilton, S.M. & Hattori, K.H. 2008. 28. Project Unit 07-025. 28. Project Unit 04-025. Detailed investigation of chemical and microbiological parameters over forest-ring edges in northern Ontario. In: *Summary of Fieldwork and Other Activities*. Ontario Geological Survey Open File Report **6226**, 28-1–28-8.
- Cameron, E.M., Hamilton, S.M., Leybourne, M.I., Hall, G.E.M. & McClenaghan, M.B. 2004. Finding deeply buried deposits using geochemistry. *Geochemistry: Exploration, Environment, Analysis*, **4**, 7–32.
- Diatreme Explorations 1999. Corporate profile and property portfolio. Diatreme Explorations Inc., Queensland, Australia.
- Dreimanis, A. 1962. Quantitative gasometric determination of calcite and dolomite by using Chittick apparatus. *Journal of Sedimentary Petrology*, **32**, 520–529.
- Dubois, J.M. 1994. *Mycological origin of rings in the coniferous forest of Anticosti Island in the Gulf of Saint Lawrence, Canada*. Photo-Interpretation 1993–3, July–August. Éditions Eska, Paris, 209–210.
- Dyke, A.S. 2004. An outline of the deglaciation of North America with emphasis on central and northern Canada. In: Ehlers, J. & Gibbard, P.L. (ed.), *Quaternary Glaciations—Extent and Chronology, Part II: North America. Developments in Quaternary Science*, **2b**. Elsevier, Amsterdam, 373–424.
- Giroux, J.-F., Bergeron, Y. & Veillette, J.J. 2001. Dynamics and morphology of giant circular patterns of low tree density in black spruce stands in northern Québec. *Canadian Journal of Botany*, **79**, 420–428.
- Govett, G.J.S. 1973. Differential secondary dispersion in transported soils and post-mineralisation rocks: An electrochemical interpretation. In: Jones, M.J. (ed.) *Geochemical Exploration, 1972*. Institution of Mining and Metallurgy, London, 81–91.
- Gregory, P.H. 1982. Fairy rings, free and tethered. *Bulletin of the British Mycological Society*, **16**, 161–163.
- Hall, G.E.M., Vaive, J.E., Beer, R. & Hoashi, M.S. 1996. Selective leaches revisited, with emphasis on the amorphous Fe oxyhydroxide phase extraction. *Journal of Geochemical Exploration*, **56**, 59–78.
- Hall, G.E.M., McClenaghan, M.B. & Hamilton, S.M. 2005. *Selective extractions – secondary geochemical signatures in glaciated terrains*. Short Course Notes; Exploration Geochemistry Workshop; Canadian Institute of Mining and Metallurgy; Mining Rocks, Prospectors and Developers Convention 2005, Toronto, April 23.
- Hamilton, S.M. 1998. Electrochemical mass-transport in overburden: a new model to account for the formation of selective leach geochemical anomalies in glacial terrain. *Journal of Geochemical Exploration*, **63**, 155–172.
- Hamilton, S.M. 2000. Spontaneous potentials and electrochemical cells. In: Govett, G.J.S. (ed.) *Geochemical Remote Sensing of the Subsurface, Handbook of Exploration Geochemistry, Volume 7*. Elsevier, 81–119.
- Hamilton, S.M. 2007. Major advances in soil geochemical exploration methods for areas of thick glacial drift cover; paper. In: Mikereit, B. (ed.) *Proceedings of Exploration 07: Fifth Decennial International Conference on Mineral Exploration*, 263–280.
- Hamilton, S.M. & Cranston, D.R. 2000. Thick overburden geochemistry – methods and case studies. In: *Summary of Fieldwork and Other Activities, 2000*. Ontario Geological Survey Open File Report **6032**, 47-1–47-8.
- Hamilton, S.M. & Hattori, K.H. 2008. Spontaneous potential and redox responses over a forest ring. *Geophysics*, **37**, B67–B75.
- Hamilton, S.M. & Govett, G.J.S. 2010. Vertical dispersion of elements in thick transported cover above the Thalanga Zn–Pb–Cu deposit, Queensland, Australia; evidence of redox-induced electromigration. In: Goldfarb, R.J., Marsh, E.E. & Monecke, T. (eds) *The Challenge of Finding New Mineral Resources; Global Metallogeny, Innovative Exploration and New Discoveries volume II; zinc-lead, nickel-copper-PGE and uranium*. Society of Economic Geologists Special Publication, **15**, 391–398.
- Hamilton, S.M., Veillette, J.J. & Komararchka, R. 1999. *A geological model to account for the formation and surprising circularity of forest rings of the James Bay basin*. Poster presented at the 1999 Prospectors and Developers Association of Canada annual meeting, Toronto, Ontario, March 16.
- Hamilton, S.M., Burt, A.K., Hattori, K.H. & Shiota, J. 2004a. The distribution and source of forest ring-related methane in northeastern Ontario. In: *Summary of Fieldwork and Other Activities, 2004*. Ontario Geological Survey Open File Report **6145**, 21-1–21-6.
- Hamilton, S.M., Cameron, E.M., McClenaghan, M.B. & Hall, G.E.M. 2004b. Redox, pH and SP variation over mineralization in thick glacial overburden – Part I: Methodologies and field investigation at Marsh Zone gold property. *Geochemistry: Exploration, Environment, Analysis*, **4**, 33–44.
- Hamilton, S.M., Cameron, E.M., McClenaghan, M.B. & Hall, G.E.M. 2004c. Redox, pH and SP variation over mineralization in thick glacial overburden – Part II: Field investigations at the Cross Lake VMS property. *Geochemistry: Exploration, Environment, Analysis*, **4**, 45–58.
- Konhauser, K. 2007. *Introduction to Geomicrobiology*. 1st edn. Blackwell Publishing, Oxford.
- Klusman, R.W. 2009. Transport of ultratrace reduced gases and particulate, near-surface oxidation, metal deposition and adsorption. *Geochemistry: Exploration, Environment, Analysis*, **9**, 203–213, <http://doi.org/10.1144/1467-7873/09-192>
- Millar, W.N. 1973. *Property report on Templeton Township property*. Timmins Resident Geologist's Office, Templeton Township Assessment File **T-2253**, 15.
- Mollard, J.D. 1980. *Landforms and Surface Materials of Canada: A Stereoscopic Atlas and Glossary*, 6th edition. Saskatchewan, Regina.
- Parra, E. & Lin, L. 2009. *Microbial fuel cell based on electrode-exoelectrogenic bacterial interface*. Proceedings IEEE MEMS Conference, Sorrento, 31–34.
- Paulen, R.C. & McClenaghan, M.B. 1998. *Surficial geology, Manning Lake northeastern Ontario*. Geological Survey of Canada Open File Report **3618**, Scale, 1:50,000.
- Pinson, W.H. Jr. 1979. Origin of Circular Ring Features in the wetlands of Ontario. *Lunar and Planetary Science*, **X**, 984–985.
- Reed, L.E. 1980. *Report on the investigation of two ring structures in the James Bay Lowlands*. Unpublished company report, Selco Mining Corporation, Toronto.
- SAS Institute Inc., 2012. Chapter 1: Principal Component Analysis. In: *A Step-by-Step Approach to Using the SAS System for Factor Analysis and Structural Equation Modeling*. SAS publishing, Cary, North Carolina, <http://support.sas.com/publishing/pubcat/chaps/55129.pdf> [last accessed 17 February 2012].
- Smith, S.L. & Burgess, M.M. 2002. *A digital database of permafrost thickness in Canada*. Geological Survey of Canada Open File **4173**, 1 CD-ROM.
- Usik, L. 1966. *A report on circular features in organic terrain*. Geological Survey of Canada, Department of Mines and Technical Surveys, Paper 66–2, Report of the Committee, November 1965–April 1966.
- Veillette, J.J. & Giroux, J.F. 1999. *The enigmatic rings of the James Bay lowland: A probable geological origin*. Geological Survey of Canada Open File Report **3708**, 28.
- Yeager, J.R., Clark, J.R., Mitchell, W. & Renshaw, R. 1998. Enzyme leach anomalies associated with deep Mississippi Valley-type zinc ore bodies at the Elmwood Mine, Tennessee. *Journal of Geochemical Exploration*, **61**, 103–112.